5592 *Biochemistry* **2009,** *48,* 5592–5601
DOI: 10.1021/bi900478b

BIOCHEMISTRY
including biophysical chemistry & molecular biology
Article

DNA-Binding Activity of the Vancomycin Resistance Associated Regulator Protein VraR and the Role of Phosphorylation in Transcriptional Regulation of the *vraSR* Operon[†]

Antoaneta Belcheva,[‡] Vidhu Verma,[§] and Dasantila Golemi-Kotra*[,‡,§,∥]

[‡]*Departments of Biology and* [§]*Chemistry, York University, Toronto, Ontario M3J 1P3, Canada, and* [∥]*Department of Chemistry and Biochemistry, University of North Carolina, Greensboro, North Carolina 27412*

Received March 19, 2009; Revised Manuscript Received May 6, 2009

ABSTRACT: In *Staphylococcus aureus* the VraSR two-component system acts as a sentinel that can rapidly sense cell wall peptidoglycan damage and coordinate a response to enhance the resistance phenotype. VraR is a transcription factor and its cognate kinase, VraS, modulates the DNA-binding activity of VraR by regulating its phosphorylation state and hence its dimerization state. Here we provide the first report on the VraR transcriptional activity by investigating the interaction with the *vraSR* operon control region. We found that this region contains three VraR-binding sites, each with unique VraR-binding features. VraR binding to the most conserved site is phosphorylation independent, and dimerization is proposed to be induced through binding to DNA. By contrast, binding to the less conserved site requires phosphorylation of VraR. This site overlaps with the binding site of the σ subunit of the RNA polymerase complex, suggesting that VraR could be interacting with the transcription machinery in the presence of the cell wall stress signal. Mutagenesis studies on the VraR binding sites suggest that there is directionality in the binding of VraR to the target DNA, probably dictated by VraR dimerization. We also constructed a P_{vraSR}-fused *lux* operon reporter vector to investigate *in vivo* the significance of our *in vitro* studies. These studies show that upon cell wall stress, induced by oxacillin, the expression level of the *lux* operon goes up and it is affected by the integrity of the two identified VraR-binding sites in agreement with the *in vitro* studies. Further, they demonstrate that the VraR most conserved binding site is essential to the *vraSR* operon expression. On the other hand, they suggest that the role of the VraR less conserved site could be that of mediating high levels of *vraSR* operon expression during cell wall stress conditions.

The two-component vancomycin resistance associated sensor/regulator (VraSR)[1] signal transduction system of *Staphylococcus aureus* coordinates the response to antibiotics that inhibit cell wall peptidoglycan biosynthesis (cell wall synthesis inhibitors) (*1*−*3*). Inactivation of *vraSR* was shown to drastically affect resistance to β-lactams and vancomycin in different *S. aureus* strains and to convert the homogeneous oxacillin resistance phenotype to a highly heterogeneous resistance phenotype (*4*). A recent study by Tomasz and co-workers linked VraSR with the biosynthesis of peptidoglycan and proposed the cross-linking event to be under the guard of this two-component system (*4*). Taken together, these observations indicate that VraSR can sense flaws in peptidoglycan integrity caused by cell wall synthesis inhibitors and coordinate the cell response to nullify the deleterious effects. Since the VraSR system has important implications in *S. aureus* antibiotic resistance and cellular responses to this insult, it is necessary to gain a molecular understanding of the mechanisms of signal transduction and gene regulation mediated by this system.

VraSR is a typical two-component system that rapidly senses and transduces cell wall stress (*2*, *5*). A recent analysis of the kinetics of the autophosphorylation of VraS and the phosphotransfer catalyzed by VraR strongly suggested that VraS may be the only biologically relevant kinase of the response regulator protein, VraR, and that the VraSR system is the main pathway through which the signal to cell wall stress response is transduced (*5*). In addition, it has been shown that phosphorylation of VraR induces dimerization, an indication that dimerization could be modulating the VraR activity (*5*).

The current work investigates the DNA-binding activity of VraR and its regulatory activities in the context of the *vraSR* operon. The work by Kuroda and co-workers showed that VraR acts as an activator of its operon (*2*). Yin and co-workers have shown that the operon control region for v*raSR* is located upstream of the operon (*6*). Recently, a DNA-binding sequence for VraR was proposed based on the structural similarities between DosR and the C-terminal domain of VraR (*7*). However, there has been no direct probing of the interactions of VraR with target operons and its transcriptional regulation mechanism.

[†]This work is supported by a grant to D.G.-K. from the Natural Sciences and Engineering Research Council of Canada.

*Address correspondence to this author at the Department of Chemistry, York University and Department of Chemistry and Biochemistry, University of North Carolina at Greensboro. E-mails: dgkotra@yorku.ca and d_golemi@uncg.edu.

[1]Abbreviations: VraSR, vancomycin resistance associated sensor/regulator; TCS, two-component system; HK, histidine protein kinase; RR, response regulator protein; EMSA, electromobility shift assays.

Published on Web 05/06/2009

Sequence alignments of VraR with other response regulators indicate that this protein belongs to the NarL/FixJ subfamily of signal transduction response regulators (*5*). These proteins use helix−turn−helix motifs to bind to DNA (*8*). Although the NarL/FixJ family members share a high sequence similarity at the C-terminus (DNA-binding domain), each of them recognizes unique DNA sequences and utilizes diverse regulatory strategies (Table 1). This could probably result from subtle differences in the primary structure of the helix−turn−helix motif (*9*) and/or tertiary structure of the active state of the response regulators (*8*). Such diversity in regulatory schemes makes it challenging to predict general gene regulation mechanisms within this family.

Herein, we report the DNA-binding sequence of VraR in the *vraSR* operon control region and the effect that phosphorylation has on the DNA-binding activity of VraR. We used *lux* operon reporter vector to investigate *in vivo* the VraR binding sites. On the basis of these findings, we propose a model of the transcriptional activation of the *vraSR* operon by VraR.

MATERIALS AND METHODS

Growth Media and Chemicals. Chemicals were purchased from Sigma or Fisher, unless otherwise stated. Chromatography media and columns were purchased from GE Healthcare. The growth media and the antibiotics were purchased from Fisher. *Escherichia coli* Nova Blue and BL21(DE3) strains, as well as cloning and expression plasmids, were purchased from Novagen. Restriction enzymes were obtained from either New England Biolabs or Stratagene. The [γ-^{32}P]ATP (6000 Ci/mmol) was purchased from Perkin-Elmer LAS Canada Inc. (Toronto, Canada) or GE Healthcare.

Isolation of the Target Proteins. Full-length VraR and its C-terminal domain (residues 141−209) were cloned into pET26b in the absence of any tags or extra amino acids. The proteins were expressed in *E. coli* strain BL21(DE3) and purified as previously described (*5*).

Phosphorylation of VraR by Acetyl Phosphate. Phosphorylation of purified VraR was carried out as previously described (*5*). Briefly, a solution of 100 μM VraR was prepared in reaction buffer (50 mM Tris−base, pH 7.4, 50 mM KCl, and 5 mM $MgCl_2$) supplemented with 50 mM lithium potassium acetyl phosphate. The reaction was incubated at 37 °C for 1 h. The extent of VraR phosphorylation was monitored by HPLC (Varian Inc.) using a ProSphere HP C4 reverse-phase column (5 μm, 300 Å, 4.6 × 250 mm) and was assessed by integrating the surface areas under the peaks corresponding to VraR-P and VraR species. Herein, VraR∼P refers to VraR solutions composed of a mixture of VraR and VraR-P. The phosphorylation of VraR under our experimental conditions is 46%.

DNase I Footprinting Assay. The DNA sequence encompassing nucleotides −121 to +26 (with respect to the transcription starting site (*6*)) of the *vraSR* operon control region (P_{vraSR}) was amplified using the PCR primers Dir, 5′-ACGAAGCTTGGTCCGATTTTAACGACAAAAATTG-3′, and Rev, 5′-TGAAATGACGCATTGATTGTGTTC-3′. For DNase I footprinting the primer of interest (Dir or Rev) was 5′-end labeled with T4 polynucleotide kinase in the presence of [γ-^{32}P]ATP (6000 Ci/mmol) and used to amplify the P_{vraSR}. Binding reactions (20 μL) were prepared in binding buffer (100 mM Tris−base, pH 7.5, 500 mM KCl, and 10 mM DTT) supplemented with 5 mM $MgCl_2$, 0.05% NP 40, 200 ng/μL poly(dI-dC), and 2.5% glycerol. The ^{32}P-end-labeled P_{vraSR} (10 ng) was mixed with VraR, VraR^C, or VraR∼P at concentrations ranging from 5 to 80 μM (VraR∼P represents a mixture of phosphorylated and unphosphorylated VraR in which the phosphorylated species typically comprised 46% of the total VraR protein). Binding reactions were incubated for 30 min at 37 °C and then subjected to DNase I (2 units) for 2 min at 25 °C. The digestion reactions were stopped by adding 50 μL of DNase I stop solution (1% SDS, 0.2 M NaCl, 20 mM EDTA, pH 8.0, and 0.25 mg/mL tRNA). Digested DNA samples were isolated by phenol−chlorophorm extraction and ethanol precipitation. They were then resuspended in formamide containing loading dye, heated at 95 °C, and loaded into an 8% polyacrylamide gel containing 7 M urea. The dried gels were either exposed to Kodak BioMax MR film and analyzed by autoradiography or scanned using a Typhoon Trio$^+$ variable mode imager (GE HealthCare). The C and G sequencing reactions for these experiments were carried out with the same end-labeled oligonucleotide, using terminator DNA polymerase, acyGTP, and acyCTP (*10*).

Table 1: DNA-Binding Sequences for Several RRs[a]

RR	sequence	mode	ref
VraR	ACTaaAGTaTGAacaTCA		this study (R1)
DosR[b]	ttGGGACTaaaGTCCCaa	6-3-6	(*30*)
NarL[b]	cgTACCCATtaATGGGTAcg	7-2-7	(*14*)
FixJ[b]	tctaaGTAGTTTCCC		(*31*)
TraR[c]	ATGTGCAGATCTGCACAT		(*32*)
LiaR[d]	ATAcGAC——GTCtTATAtAAAAA	7-4-7	(*19*)
CesR[d]	TCAGTC—AGTCTGA	7-3-7	(*18*)
OmpR[b]	tTTACtTtTgGTTACA*t*att		(*33*)
PhoP[b]	(T/G)GTTA———(T/G)GTTA	6-5-6	(*34*)

[a] All but OmpR and PhoP belong to the NarL/FixJ family of proteins. [b] The consensus binding site identified experimentally; uppercase letters are the conserved residues. [c] Binding sequence identified through DNase I. [d] *In silico* determination of the consensus binding site.

Electromobility Shift Assays. The DNA-binding activities of VraR, VraR∼P, and VraR^C to target DNA were analyzed by electromobility shift assays (EMSA). The short double-stranded DNA sequences were prepared by primer annealing (Table 1 in Supporting Information). Typically, annealing reactions were carried out in 50 μL reactions containing equal amounts of the complementary synthetic oligonucleotides (1 μg/μL), 5 μL of 10× annealing buffer (100 mM Tris, pH 7.5, 500 mM NaCl, and 10 mM EDTA), and nuclease-free water. The samples were heated at 95 °C for 2 min and then were allowed to cool to 4 °C. The formed duplex sequences were separated from single-stranded DNA by purification in a 10% native polyacrylamide gel. The resulting double-stranded DNA sequences were labeled using T4 polynucleotide kinase using [γ-^{32}P]ATP (3000 Ci/mmol). Binding reactions (20 μL) were prepared in binding buffer (10 mM Tris−base, pH 7.5, 50 mM KCl, and 1 mM DTT) supplemented with 5 mM $MgCl_2$, 0.05% NP 40, 200 ng/μL poly(dI-dC), and 2.5% glycerol. Target DNA (2 ng) was mixed with protein concentrations varying from 1 to 25 μM or up to 40 μM for VraR^C. In our experiments VraR∼P represents a mixture of phosphorylated and unphosphorylated VraR in which the phosphorylated species typically comprised 46% of the total VraR protein. The reaction mixtures were incubated at 25 °C for 30 min and loaded into a 10% native polyacrylamide gel (the incubation time was determined based on the time required for the equilibrium to be set for the sample with the lowest protein concentration). Dried polyacrylamide gels were analyzed by a Packard instant imager (a Canberra Co.,

Meriden, CT) or Typhoon Trio$^+$ variable mode imager (GE HealthCare). The incubation time was determined experimentally as the time required for the equilibrium to be reached at the smallest VraR (VraR∼P and VraR^C) concentration used in these assays. These experiments were repeated at least three times. The dissociation constants were determined from the nonlinear regressional analysis of the experimental data using the binding equation % DNA bound = Cap[P]^n/($K_d{}^n$ + [P]^n), where n is the Hill coefficient, Cap is the binding capacity, and [P] is the protein concentration in the assay.

Construction of the luxABCDE Fusion Strains Using Variants of vraSR Operon Control Region. The *lux* reporter vector hosts the promoterless *lux* operon from *Photorhabdus luminescens* (*11*). It was constructed by Francis et al. to study *in vivo* the activity of target promoters. The *lux* operon is composed of five structural genes *lux* A−E that mediate the synthesis of the bioluminescent substrate and luciferase (*luxAB*). Upstream of the *lux* operon is inserted a multiple cloning site to aid fusion of the promoter of interest to the *lux* operon. Each structural gene in the *lux* operon is fused to the ribosomal binding site that is characteristic of *S. aureus* in order to facilitate their expression in Gram-positive bacteria. Two DNA sequences derived from the *vraSR* operon control region, encompassing nucleotides −462 to +150 (this region was recently investigated by the *lacZ* reporter vector (*12*)) and −121 to +26, were amplified by PCR using the genomic DNA of *S. aureus* RN4220 as a template. The primers designed to amplify the −462 to +150 region ($P_{vraSR}{}^L$) were designed to introduce the *Eco*RI and *Bam*HI restriction sites at the 5′ and 3′ ends, respectively: Dir_$P_{vraSR}{}^L$-5′-*AGGAATT*-*C*ATGGCATTTGAGAATGCA-3′ and Rev_$P_{vraSR}{}^L$-5′-CG*GGATCC*ACGTTCAACATAGTTCATAAC-3′ (the restriction sites are italicized) . The primers designed to amplify the −121 to +26 region (P_{vraSR}) were also designed to introduce the *Eco*RI and *Bam*HI restriction sites at the 5′ and 3′ ends, respectively: Dir_P_{vraSR}-5′-AG*GAATTC*GGTCCATTTTAACGACAAAAATTG-3′ and Rev_P_{vraSR}-5′-CG*GGATCC*TGAAATGACGCATTGATTGTGTTC-3′. The amplicons were ligated into the blunt end vector pSTBlue-1 using the cloning kit from the vendor (Novagen). The ligation mixtures were introduced into *E. coli* DH5α by heat shock, and the transformants were plated into LB−agar plates supplemented with 100 μg/mL ampicillin and 20 μg/mL X-gal for white and blue screening. The putative positive recombinant clones were confirmed by sequencing the plasmid for the presence of the insert. The pSTblue-1: P_{vraSR} plasmid was used as a template for generation of two P_{vraSR} mutants carrying the same mutation as in R1-DM3 and R2-SM1, respectively. These amplicons are referred to as $P_{vraSR}{}^{R1\text{-}DM3}$ and $P_{vraSR}{}^{R2\text{-}SM1}$, respectively.

We used the QuickChange mutagenesis kit from Stratagene to carry out the mutations. The mutagenic primers were Dir_$P_{vraSR}{}^{R2\text{-}SM1}$-5′-TTAGTTCCGGAA**C**CTATTCATATTGGT-3′ and Rev_$P_{vraSR}{}^{R2\text{-}SM1}$-5′-ACCAATATGAATAGG**T**TCCGGAACTAA-3′; Dir_$P_{vraSR}{}^{R1\text{-}DM3}$(1)-5′-CAACATATACTAAGA**T**TAAAGTATGAACATC-3′ and Rev_$P_{vraSR}{}^{R1\text{-}DM3}$(1)-5′-GATGTTCATACTTTAA**T**CTTAGTATATGTTG-3′; Dir_$P_{vraSR}{}^{R1\text{-}DM3}$(2)- 5′- ATACTAAGATTAAA**T**TATGAACATC-ATTTAG-3′ and Rev_$P_{vraSR}{}^{R1\text{-}DM3}$(2)-5′-CTAAATGATGTTCATAA**T**TTAATCTTAGTAT-3′ (the mutations in R1 were carried out in two steps; the replaced nucleotides are highlighted). After mutagenesis the DNA fragments were excised from the pSTBlue-1 fusion plasmids using the restriction enzymes *Eco*RI and *Bam*HI. The fragments were gel purified and each ligated into the pXEN1 vector that was digested also with the above restriction enzymes. The ligation mixtures were introduced into the *E. coli* DH5α strain, and the transformants were plated on Luria−Bertani (LB)−agar plates supplemented with 100 μg/mL ampicillin (selection marker in pXEN1). The putative positive colonies were confirmed to harbor the inserts by sequencing the plasmid with one primer derived from the *luxA* sequence, 5′-GTAAGCAAAAGTTTCCAAATTTCAT-3′, and the forward primer used to amplify the insert. The pXEN1 plasmid carrying the $P_{vraSR}{}^L$, P_{vraSR}, $P_{vraSR}{}^{R1\text{-}DM3}$, or $P_{vraSR}{}^{R2\text{-}SM1}$ insert is referred to as the *lux* fusion plasmid ($P_{vraSR}{}^L$::*lux*, P_{vraSR}::*lux*, $P_{vraSR}{}^{R1\text{-}DM3}$::*lux*, $P_{vraSR}{}^{R2\text{-}SM1}$::*lux*).

The pXEN1 plasmid and *lux* fusion plasmids were introduced into the restriction-deficient *S. aureus* strain RN4220 by electroporation (*13*). The transformants were plated on tryptic soy broth (TSB)−agar plates supplemented with 10 μg/mL chloramphenicol (selection marker in pXEN1). The putative positive colonies were confirmed by sequencing of the plasmids using the primers described above. The *S. aureus* RN4220 carrying the empty vector pXEN1 is referred to as RN(::*lux*), and *S. aureus* RN4220 carrying one of the *lux* fusion plasmids is referred to as *lux* fusion strain: RN($P_{vraSR}{}^L$::*lux*), RN(P_{vraSR}::*lux*), RN($P_{vraSR}{}^{R1\text{-}DM3}$::*lux*), and RN($P_{vraSR}{}^{R2\text{-}SM1}$::*lux*).

The effect of pXEN1 and *lux* fusion plasmids on the growth of *S. aureus* was investigated by monitoring the bacterial growth profile for all the strains. Briefly, *lux* fusion strains, RN(::*lux*) and RN4220, were inoculated into TSB and grown overnight with 5 μg/mL chloramphenicol, with the exception of the wild-type strain, at 37 °C. Next, 1% culture was inoculated in fresh TSB supplemented with 5 μg/mL chloramphenicol except for RN4220. Then the OD (620 nm) of the cell culture of all the strains was measured at 1 h intervals for the next 6 h.

Measurement of Bioluminescence from S. aureus Strains. After overnight growth, the wild-type strain and the strains harboring the *lux* fusion plasmids and pXEN1 were diluted into fresh TSB and grown further at 37 °C and with shaking at 200 rpm. The strains were grown to an OD ∼ 0.3 and then subjected to oxacillin at 1.2, 10, and 100 μg/mL for 2 h. The optical densities were measured at 620 nm for all the samples. The cell cultures with higher OD were diluted such that the cell density in each cell culture was the same. A 300 μL aliquot from each sample (in triplicate) was transferred to an opaque 96-well optiplate and analyzed in a HT-Analyst (Molecular Devices, Sunnyvale, CA). Bioluminescence was measured immediately after dispensing the samples into the plates. The signal was measured for 1 min over a period of 20 min with integral measurement for 1 s at 1 mm luminescence height. The data points collected over 20 min were averaged for each strain and oxacillin concentration, and the standard deviations were determined from three independent measurements.

Viability Test of the Cultures. A 1% of overnight grown seed cultures of the wild-type strain, *lux* fusion strains, and RN(::*lux*) were inoculated in TSB containing 5 μg/mL chloramphenicol. When the OD of the cell cultures reached ∼0.3, oxacillin was added to each culture to a final concentration of 1.2, 10, or 100 μg/mL, and the cell cultures were grown for an additional 2 h. The OD of each culture was normalized to the samples having the lowest OD. A 20 μL aliquot from each uninduced and induced cell culture was diluted 10000-fold using TSB to remove the antibiotic. Then a 50 μL aliquot from each of these diluted cell cultures was plated on TSB−agar plates, without antibiotic. Cells were allowed to grow at 37 °C. These experiments were repeated three times.

FIGURE 1: An overview of the *vraSR* operon composition in the *S. aureus* strain Mu50. Highlighted are the structural genes in the *vraSR* operon (gray arrows), transcription starting point (tsp), the operon control region used in this study, and the neighboring *map* gene.

RESULTS

DNase I Footprinting. The P_{vraSR} region spanning from −121 to +26 (Figure 1) was subjected to DNase I in the presence and absence of VraR, $VraR^C$ (C-terminal domain of VraR), and VraR∼P to identify the VraR-binding site(s) and its mode of binding. These experiments were carried out using ^{32}P-end-labeled top or bottom strand DNA (Figure 2). Unphosphorylated VraR and $VraR^C$ showed similar DNase I protection of P_{vraSR} but differed from VraR∼P (Figure 2). The DNase I protection of the top strand by VraR proteins consists of one single protected site, unlike the bottom strand where we observed distinct protected sites. Two distinct DNA-binding sites could be deduced for VraR and $VraR^C$ in the bottom strand, each spanning the regions −77 to −71 and −68 to −52. In the top strand, the single protected site spanned the region from −75 to −50. In addition, two hypersensitive sites were introduced by VraR and $VraR^C$ in the bottom strand, −75 and −62, which were absent in the top strand (Figure 2). These observations indicate that VraR contacts both DNA strands, but it may interact more closely with the top strand. Alternatively, the bound protein may be involved in protein−protein interactions as a result of which certain regions of the target DNA in the top strand are excluded from DNase I and/or they become more accessible in the bottom strand possibly due to DNA bending (*14*).

The effect of the VraR phosphorylation on the DNase I protection profile was dramatic (Figure 2), considering that only 46% of VraR is phosphorylated. At first glance, the DNase I protection profile of VraR∼P indicates four major effects of phosphorylation on the VraR DNA binding activity. First, DNA binding affinity of VraR for both DNA strands is enhanced. Second, DNase I protection of P_{vraSR} is extended upstream of −77. Third, phosphorylation caused a downstream shift in the hypersensitive site on the bottom strand (from −75 to −72) and the appearance of a new hypersensitive site at −68. Finally, a new DNA-protected region, located between positions −46 and −26, emerged. Because the phosphorylated VraR samples (VraR∼P) contain a mixture of phosphorylated and unphosphorylated VraR protein (only 46% of VraR is phosphorylated), these observations strongly indicate that differences in the P_{vraSR} DNase I footprinting between VraR and VraR∼P are a consequence of VraR phosphorylation.

The VraR-Binding Sites in P_{vraSR}. The analysis of DNase I footprinting assays shows that VraR binds to three different regions in P_{vraSR}: −68 to −52 (R1), −46 to −25 (R2), and −90 to −71 (R3). The DNase I protection at these sites took place at different protein concentration, and each protein displayed a different protection pattern, indicating that these sites have unique features. The R1 site, in both strands, is protected by the three proteins, though at different levels. In the case of the R3 site, binding of VraR and $VraR^C$ produced the same DNase I protection pattern on the bottom strand and introduced a hypersensitive site at position −75. No protection or hypersensitive sites were observed in the top strand by these proteins at R3.

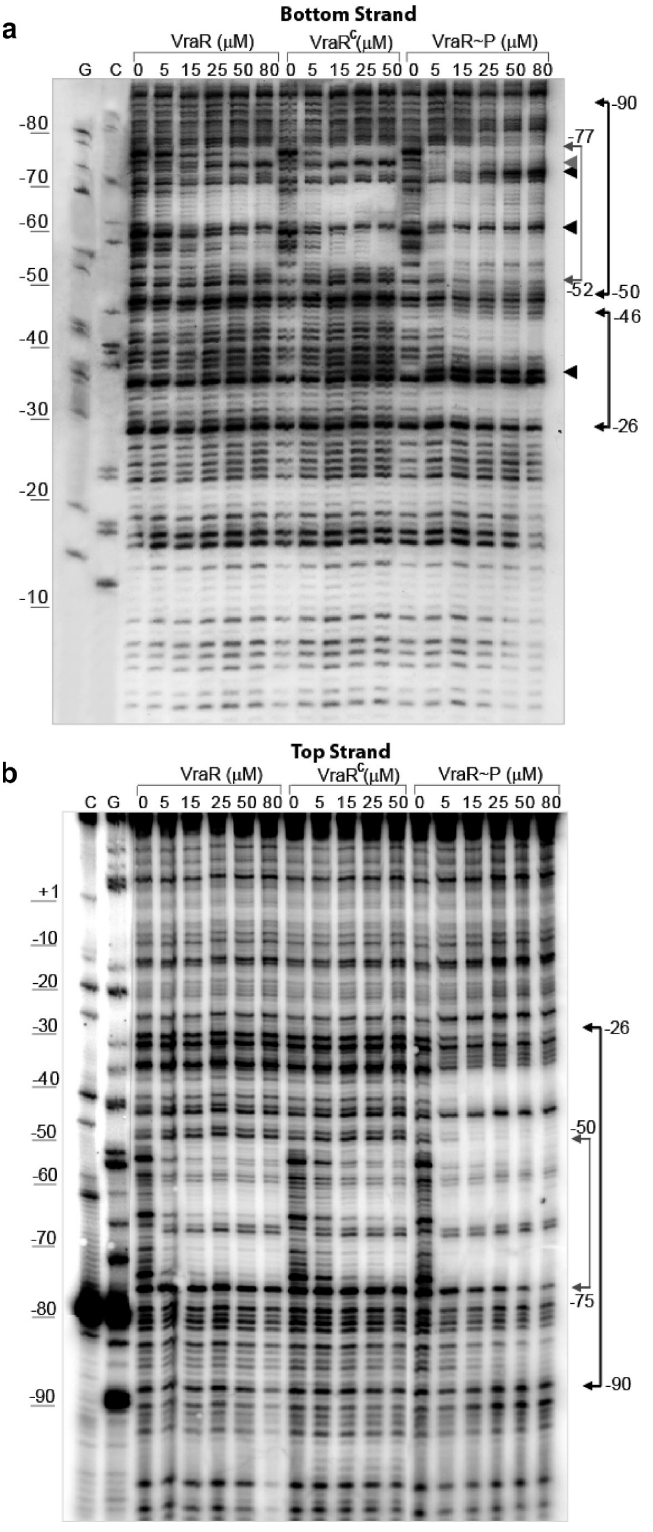

FIGURE 2: DNase I footprint of the P_{vraSR} with VraR, $VraR^C$, and VraR∼P. (a) The bottom DNA strand. (b) The top DNA strand. The G and C sequencing reactions were calibrated with respect to the number of base pairs from the transcription starting point. In gray lines are highlighted the regions protected by VraR and $VraR^C$, and in solid lines are highlighted the regions protected by VraR∼P. Arrowheads indicate the hypersensitive sites.

Only phosphorylation introduced protection at this site in the top strand. In addition, phosphorylation caused a downstream shift in the hypersensitive site on the bottom strand (from −75 to −72) and the appearance of a new hypersensitive site at −68. By contrast, the R2 site, on both strands, is protected only by

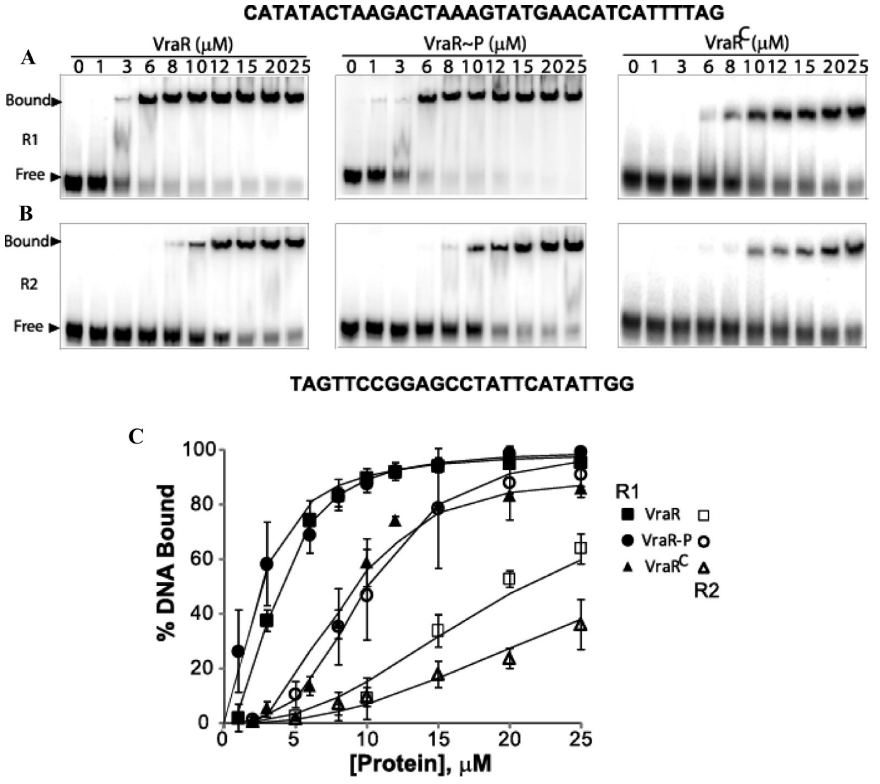

FIGURE 3: Analysis of the DNA-binding activities of VraR, VraR^C, and VraR~P by EMSA. (A) Binding of these proteins to the R1 site. (B) Binding of the above proteins to the R2 site. (C) Binding isotherms of VraR (squares), VraR^C (triangles), and VraR~P (circles) to the R1 (solid geometric shapes) and R2 sites (empty geometric shapes). In a typical assay, 2 ng of 5′-γ-^{32}P-end-labeled P_{vraSR} was incubated with different concentrations of VraR proteins for 30 min at 25 °C (the standard deviations calculated from three independent experiments do not exceed 10% of each data point).

Table 2: Determination of the Dissociation Constants of VraR, VraR~P, and VraR^C with R1, R2, and Their Variants[a]

	VraR		VraR~P		VraR^C	
DNA sequence	K_d (μM)	n	K_d (μM)	n	K_d (μM)	n
R1	4.0 ± 0.4	2.1 ± 0.2	2.7 ± 0.9	1.9 ± 0.6	9.0 ± 0.7	3.3 ± 0.2
R1-DM1	25 ± 1	2.0 ± 0.2	16 ± 2	3.0 ± 0.5	ND[b]	ND
R1-DM2	23 ± 1	2.4 ± 0.3	7.5 ± 0.4	2.1 ± 0.1	ND	ND
R1-DM3	29 ± 1	2.6 ± 0.4	17 ± 1	3.1 ± 0.6	ND	ND
R1-DM4	9 ± 1	2.3 ± 0.2	6.3 ± 0.6	2.5 ± 0.1	ND	ND
R2	18 ± 2	3.0 ± 0.4	10 ± 1	3.5 ± 0.1	25 ± 1	2.8 ± 0.6
R2-SM1	34 ± 8	3.0 ± 0.1	24 ± 3	3.1 ± 0.4	ND[b]	ND
R2-SM2	> 40[c]	2	20 ± 4	2.7 ± 0.3	ND	ND
R2-DM1	> 40[c]	2	25 ± 5	2.6 ± 0.2	ND	ND
R2-DM2	> 40[c]	2	27 ± 9	3.0 ± 0.3	ND	ND
P_{vraSR}	4.7 ± 0.3	1.7 ± 0.1	1.4 ± 0.5	2.0 ± 0.3		
$P_{vraSR}^{R1\text{-}DM3}$	9.0 ± 0.2	1.8 ± 0.2	6.2 ± 0.3	3.0 ± 0.3		
$P_{vraSR}^{R2\text{-}SM1}$	4.0 ± 0.3	2.0 ± 0.1	3.0 ± 0.2	2.0 ± 0.1		

[a] VraR~P samples represent a mixture of VraR and VraR-P, where VraR-P constitutes only 46% of the protein mixture. Hence, the K_d values do not represent absolute dissociation constants for VraR-P. [b] The EMSA data could not be fitted due to low levels of DNA−protein complex formed at protein concentrations as high as 40 μM. [c] The K_d values could not be determined accurately due to lack of experimental data points beyond 40 μM.

VraR-P, and binding of the phosphorylated protein introduced a hypersensitive site on the bottom strand at position −36.

The quantitative analysis of the EMSA data obtained with VraR, VraR~P, and VraR^C and R1 and R2 shows that these proteins bind with higher binding affinity to R1 than R2 (Figure 3A,B and Table 2), in agreement with the DNase I footprinting assays. Interestingly, all of the binding isotherms indicate a clear positive cooperativity in binding (Figure 3C). In addition, the EMSA data indicate that VraR and VraR~P bind to R1 with similar binding affinities. By contrast, unphosphorylated VraR bound only 50% of R2 at concentrations as high as 20 μM (this could explain the lack of DNase I protection observed at this region), whereas phosphorylation of VraR enabled binding of more than 80% of R2 at this concentration, although VraR-P constitutes only 46% of VraR in these experiments. On this regard, we expect VraR-P to bind with higher binding affinity to this site. On the other hand, VraR^C bound to the R1 site weaker than VraR, but the difference in the binding affinities between VraR^C and VraR were less pronounced for the R2 site (Table 2).

The VraR binding to R3 was not investigated because the sequence has a low melting point and we were not able to prepare high-quality samples of the double-stranded DNA by

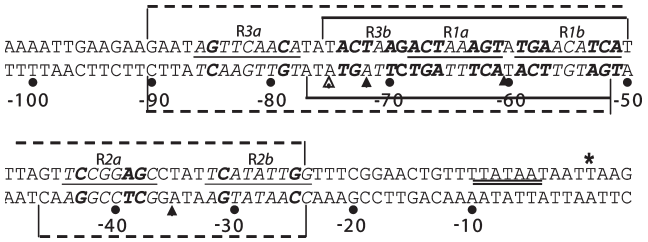

FIGURE 4: A close-up view of the VraR-binding sites on P_{vraSR}. The DNase I protection by unphosphorylated VraR for both DNA strands is shown in solid brackets. The DNase I regions protected by the phosphorylated VraR are shown in dashed brackets. The putative VraR-binding sequences are underlined, and the nucleotides proposed to be essential to the VraR recognition and binding are highlighted in bold. The transcription starting point is denoted by an asterisk, and the −10 box sequence is underlined. The black arrowheads indicate the hypersensitive site that emerges with binding of VraR∼P, and the white arrowhead indicates the hypersensitivity that emerges with binding of VraR.

primer annealing. Introduction of GC base pairs in the 5′- and 3′-ends in order to increase the thermal stability of this sequence was not considered of the concern that they may introduce bias in binding (see below). Nonetheless, the DNase I footprinting experiments indicate that VraR does not protect this region unless it is phosphorylated (the DNase I footprinting data show that 50% of protection at this site takes place at 25 μM VraR∼P).

Elucidation of the VraR-Specific Binding Sequence. Looking closely at the DNA sequences protected by VraR, VraR∼P, and VraR^C in the R1 site, we identified two putative binding sequences, separated from each other by one nucleotide: $^{-68}$*ACT*aa*AGT*$^{-61}$ (R1a) and $^{-59}$*TGA*aca*TCA*$^{-51}$ (R1b) (Figure 4). These sequences are quasi-palindromic and mirror images of each other. Within the R2 site, we also identified two potential VraR binding sequences: $^{-45}$T*C*Cgg*AG*C^{-37} (R2a) and $^{-32}$T*C*AtatT*G*G^{-24} (R2b) (Figure 4). In this case, the two sequences are separated from each other by four nucleotides. Within the R3 site, we also identified two sequences that were protected from the DNase I digestion: $^{-86}$*AGT*tcaa*CA*$^{-79}$ (R3a) and $^{-74}$*ACT*a*AG*$^{-69}$ (R3b) (Figure 4). The palindromic nature of the putative VraR-binding sequences in R2 and R3 is not completely conserved, which could explain the lack of and the weak DNase I protection observed at these sites, respectively.

Comparison of the above identified VraR DNA-binding sequences revealed that two nucleotides in particular, the C in the ACT and G in the AGT motifs, could be important recognition and/or binding elements for VraR. Interestingly, these two nucleotides are found either four or five residues apart in R1a/R2a and R1b/R2b, respectively. To investigate the roles of the cytosine and guanosine in binding of R1 and R2 to VraR, we constructed mutants of the R1 and R2 sites, in which these residues were mutated to A or T (Figure 5A) either one at a time or simultaneously, and investigated their binding affinities to VraR, VraR∼P, and VraR^C by EMSA.

Replacement of cytosines −67 and −52 by thymine in R1 (R1-DM1) completely depleted the binding of VraR^C to R1 and reduced the binding affinity of VraR and VraR∼P by ∼6-fold (Table 2, Figure 5B,D,F). Replacement of guanosines −62 and −58 with thymine in R1 (R1-DM2) had a similar effect on the binding of VraR^C and VraR to R1 (Figures 3 and 5B,F). But these mutations, unlike the ones in R1-DM1, had a lesser effect on the binding of VraR∼P to R1; a 3-fold decrease in K_d was measured, instead (Table 2, Figure 5D).

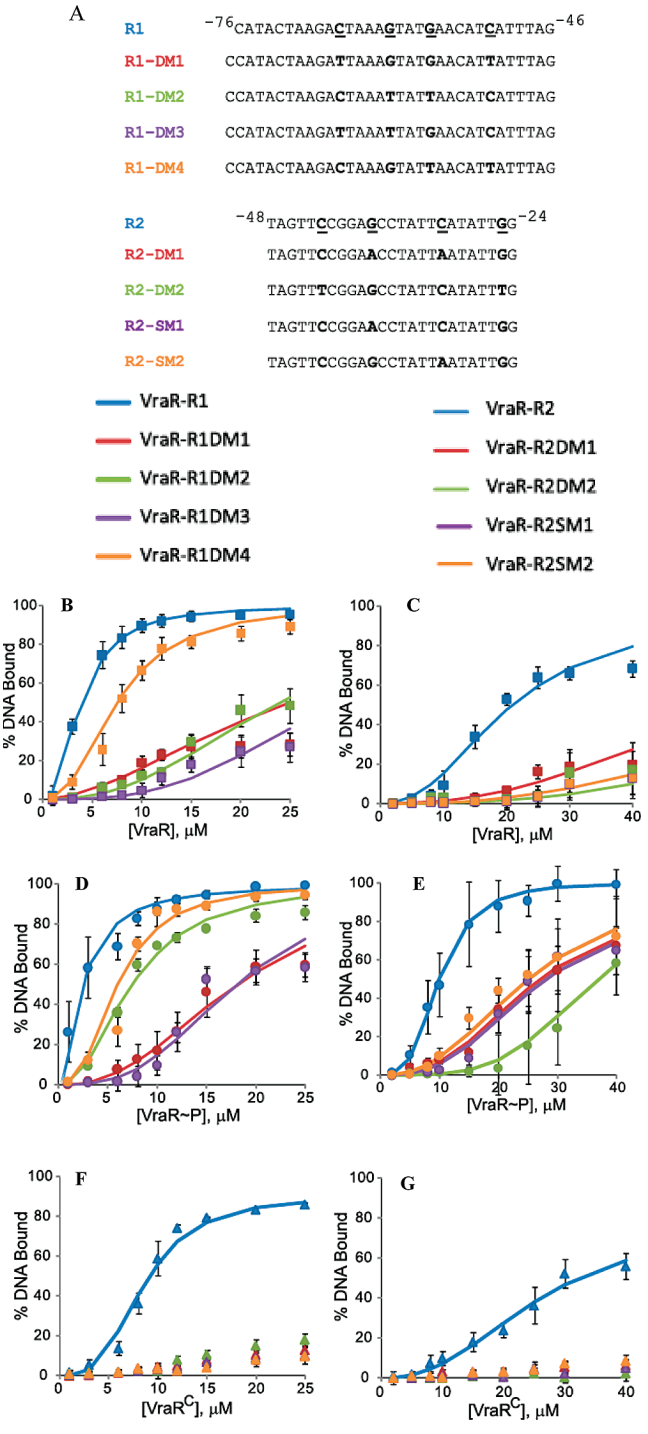

FIGURE 5: EMSA analysis of the DNA-binding activities of VraR, VraR∼P, and VraR^C to R1, R2, and their variants. (A) The DNA binding sequences of R1, R2, and their variants. (B) Binding isotherms of VraR with R1 and its variants. (C) Binding isotherms of VraR with R2 and its variants. (D) Binding isotherms of VraR∼P with R1 and its variants. (E) Binding isotherms of VraR-P with R2 and its variants. (F) Binding isotherms of VraR^C with R1 and its variants. (G) Binding isotherms of VraR^C with R2 and its variants. In a typical assay, 2 ng of 5′-γ-^{32}P-end-labeled P_{vraSR} was incubated with different concentrations of VraR proteins for 30 min at 25 °C (the standard deviations were calculated from three independent experiments).

To assess the difference in the binding affinities between R1a and R1b, we generated two other R1 double mutants: C-67/G-62 (R1-DM3) and G-58/C-52 (R1-DM4). The analyses of the EMSA data show that the removal of the R1a site (R1-DM3)

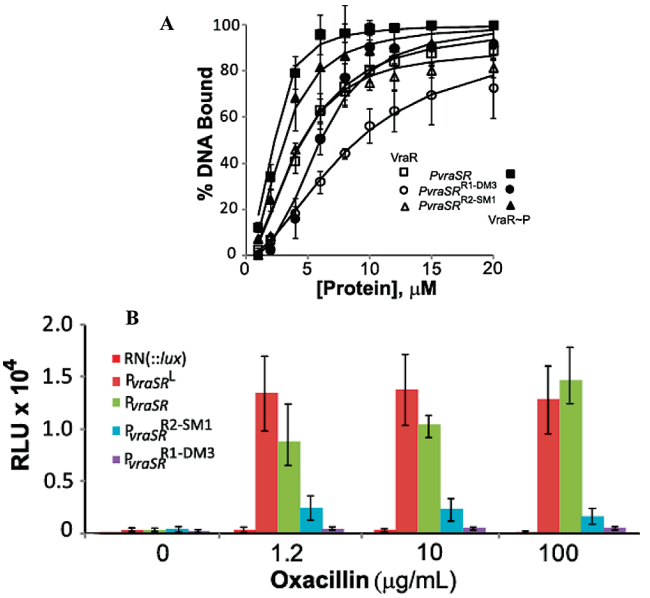

FIGURE 6: *In vivo* and *in vitro* investigation of the role of the R1 and R2 sites in the transcriptional mechanism of VraR. (A) The binding isotherms obtained from EMSA with VraR and VraR~P with P_{vraSR}, $P_{vraSR}^{R1\text{-}DM3}$, and $P_{vraSR}^{R2\text{-}SM1}$. (B) Shown are the luminescence signals obtained from all *S. aureus* strains in the presence of 1.2, 10, and 100 μg/mL oxacillin. Each strain is represented by the name of the promoter fused upstream of the *lux* operon in the pXEN1 plasmid.

decreased the binding affinity of VraR and VraR~P to R1 by 7- and 6-fold, respectively (Table 2, Figure 5B,D). By contrast, the removal of the R1b site (R1-DM4) decreased the binding affinity of VraR and VraR~P only by 2-fold (Table 2, Figure 5B,D). These results indicate that VraR binds stronger to R1a and this subsite may serve to anchor the monomeric or dimeric form of VraR to the R1 site. On the other hand, R1-DM3 and R1-DM4 displayed very low binding affinities for $VraR^C$, similarly to the R1-DM1 and R1-DM2 mutants (Table 2). It is noteworthy that in all of the cases the binding isotherms indicate a clear positive cooperativity in binding of VraR and VraR~P to R1 (Table 2). This observation suggests that binding of VraR to R1a could enhance binding of a second VraR molecule to R1b. This could be possible either through local changes in the DNA topology or through positioning of one monomer for efficient dimerization when a second monomer binds to the DNA.

To confirm the essential nature of residues C-43, G-38, C-31, and G-25 in R2, we mutated them to A or T (Figure 5A). The analysis of the EMSA data shows that double mutations C-43/G-25 (R2-DM2) and G-38/C-31 (R2-DM1) drastically reduced the binding of VraR to the R2 site (Figure 5C). Moreover, the single point mutation at G-38 and G-31 completely depleted the binding of VraR to R2 (Figure 5C,E). These results indicate that R2 is composed of two VraR-binding sequences, R2a and R2b. Also, these mutants display a positive cooperativity in binding to VraR.

The Role of R1 and R2 in Recruiting VraR to P_{vraSR} as Assessed by the lux Reporter Vector. To investigate *in vivo* the role of the R1 and R2 sites in recruiting VraR into the *vraSR* promoter region when *S. aureus* is subjected to cell wall stress, we fused P_{vraSR} upstream of the *lux* operon reporter vector pXEN1 (*11*) and constructed variants of P_{vraSR} carrying the same mutations as in R1-DM3 and R2-SM1 (the EMSA data show that VraR-P binds stronger to the R1a and R2a sites), herein referred to as $P_{vraSR}^{R1\text{-}DM3}$ and $P_{vraSR}^{R2\text{-}SM1}$. All of the *lux* fusion plasmids were introduced successfully into *S. aureus* RN4220. We also introduced the empty vector pXEN1 into *S. aureus* RN4220 to use it as a control in these experiments. In addition, as a positive control for the bioluminescent experiments we fused the P_{vraSR}^{L} into pXEN1. This sequence was shown by Steidl et al. in their *lacZ* fusion strain study to respond to oxacillin in a dose-dependent manner (*12*).

The presence of the pXEN1 or *lux* fused plasmids did not affect the growth of *S. aureus* (data not shown). In addition, the viability experiments (CFU) showed that the effect of oxacillin on the bacterial growth is the same for all of the strains (data not shown). We also determined by EMSA the binding affinities of the $P_{vraSR}^{R1\text{-}DM3}$ and $P_{vraSR}^{R2\text{-}SM1}$ sequences to VraR and VraR~P (Table 2, Figure 6A). Mutation of the R1a site reduced the binding affinity of VraR~P for P_{vraSR} by 4.4-fold, while mutation of the R2a site reduced the binding affinity of VraR~P for P_{vraSR} by 1.3-fold and decreased the occupancy of this sequence by 20% (Figure 6A).

The luminescence data collected from all of the strains are presented in Figure 6B. The data were corrected for the background signal (growth medium). In the absence of oxacillin, all of the strains exhibited very low levels of luminescence which were indistinguishable from the noise level of these experiments. The presence of oxacillin increased the luminescence signal for RN (P_{vraSR}::lux) and RN(P_{vraSR}^{L}::lux) by ~60-fold. The results obtained with RN(P_{vraSR}^{L}::lux) are in agreement with the results obtained with the *lacZ* reporter vector (*12*). The mutation of the R1a site reduced the luminescence by 17-fold at 1.2 μg/mL oxacillin. On the other hand, the mutation of the R2 site reduced the luminescence by 4-fold, at the same concentration of oxacillin.

DISCUSSION

The central role of the VraSR system in the *S. aureus* response to cell wall stress has been well documented, but the mechanism by which the stress is sensed and genes are activated remains unclear. Two recent studies utilizing a *lacZ* report vector have shown that the operon control region of *vraSR* harbors the regulatory elements of its expression (*6*, *12*). However, evidence for specific binding of VraR to the upstream regions of this operon or others has not been shown. Herein, we undertook the study to determine the VraR binding sequence and investigate the role of phosphorylation in recognition and activation of the *vraSR* operon.

We show that VraR binds to specific regions in P_{vraSR}. Analysis of the DNase I footprinting of P_{vraSR} indicates that VraR binds to three distinct sites in P_{vraSR} which are centered on positions −76 (R3), −60 (R1), and −35 (R2) (Figures 2 and 4). It is clear from these experiments that phosphorylation expands VraR binding to the −76 and −35 regions. A similar phenomenon has also been reported for other response regulators such as PhoP of *Bacillus subtilis*, BvgA of *Bortedella pertusis*, and VanR of *Enterococci faecium* but not in the case of NarL (*15*−*17*).

Based on the DNase I footprinting, EMSA, mutagenesis, and *in vivo* studies, we identified the sequence 5′-ACT(X)$_n$AGT-3′ as the VraR-specific binding sequence, where X could be any nucleic acid and *n* may vary from 1 to 3 (Figure 4). Comparison of this sequence with the DNA-binding consensus sequences (*in silico* determination) of VraR orthologues such as CesR in *Lactococcus lactis* (*18*) and LiaR in *B. subtilis* (*19*) (Table 1), both involved

with cell wall stress response in the above organisms, indicates that there are similarities between VraR and CesR DNA-binding sequences but not with LiaR, as expected (*18*). Both the CesR and VraR DNA-binding sequences share the AGT motif. Although the primary sequence alignments classify VraR as a member of the NarL/FixJ family, this protein does not share significant similarities in its DNA-binding sequence with any of the members of this family (Table 1). However, this is to be expected as there is no apparent DNA-binding consensus sequence among the NarL/FixJ members (Table 1). This could be a result of subtle differences in the primary sequence among their DNA-binding domains (*9*).

The DNA-binding sequence proposed for VraR, based on the comparison of $VraR^C$ structure with DosR−DNA complex (*7*), 5′-$^{-71}$AAGACT^{-66}-3′, does not match entirely with the DNA-binding sequence determined experimentally in this study. The DNase I footprinting, mutagenesis, and *in vivo* studies (see below) unambiguously indicate that the VraR-binding sequence is $ACT(X)_nAGT$ (Figure 4).

Analysis of the EMSA data indicates that there is a hierarchy in binding among the VraR-binding sites in P_{vraSR}; VraR (VraR-P) binds with the highest binding affinity to the R1 site and the lowest to the R2 site (Table 2). In addition, both EMSA and DNase I footprinting data suggest that there is a difference in the requirements for VraR phosphorylation for binding to R1 and R2. VraR binds to R1 with similar affinity as the phosphorylated protein, suggesting that binding of VraR to the R1 site could be phosphorylation independent. By contrast, the phosphorylation of VraR is essential for recognition and binding to the R2 site (Figure 2B). These differences suggest that the R1 site could serve to recruit VraR (VraR-P) to the P_{vraSR}, thereby increasing its local concentration and its chances for binding to weaker sites such as R2 and probably R3. This model allows occupancy of the weaker binding sites at a lower cytoplasmic concentration of VraR. This proposal is supported well by the *lux* reporter studies, whereby mutation in the R1a site greatly reduces the *lux* operon expression (a 17-fold decrease). However, mutation of the R2a site brought only a 4-fold reduction in the *lux* operon expression. It is noteworthy that the effects that mutations in R1a and R2a have on the *lux* reporter vector studies are the same as the effects observed in the binding affinities of VraR∼P for P_{vraSR}. Mutations in the R1a and R2a sites decreased the binding affinity for VraR∼P by 4.4- and 2.2-fold, respectively, which *in vivo* translated into a 17- and 4-fold effect. The *in vivo* "enhancement" of the effects that the above mutations have *in vitro* indicates that there could be a communication between these two sites in the context of the full-length P_{vraSR}, whereby binding of VraR-P into one site could affect the binding in the other site(s). In addition, because the R1 site displays the highest binding affinity for VraR-P, it could serve to recruit VraR-P to other sites in P_{vraSR}, and as such it is plausible that its loss will have overall a bigger effect in the binding of VraR-P to the promoter.

A closer investigation of the roles of the C and G residues in the VraR binding to the sequence $ACG(X)_nATG$ (n = 2 or 3) revealed that these residues are essential for VraR binding. Moreover, the data indicate that the cytosine residue has a recognition role in addition to that of binding, which in turn suggests that there is directionality in the binding of VraR to this sequence. This is relevant when considering that the apparent palindromic nature of the VraR DNA-binding sequence could give rise to a nondiscriminatory interaction between VraR and either DNA strand. *In vivo* this situation is not desirable as both strands would compete for binding to VraR, resulting in an apparent low binding affinity and an overall decrease in occupancy of the target DNA. Indeed, we observed that $VraR^C$ persistently bound with lower binding affinity to all of the sites and their derivatives, and it was not able to provide 100% occupancy of the target DNA. In addition, the presence of two and in tandem VraR-binding sequences within the R1 and R2 sites suggests that VraR could bind to these sites as a dimer, through dimerization at the N-terminal domain, which infers that directionality in DNA binding by VraR might be required to facilitate dimerization.

The observation that phosphorylation does not affect the binding of VraR to R1 suggests that unphosphorylated VraR could bind as a dimer to this site and that dimerization could be induced by binding to the target DNA. This is possible if binding to DNA brings two VraR monomers into proximity and with their dimerization interface facing each other. This proposal is supported by our observations that the removal of the N-terminal domain, which harbors the dimerization interface in VraR-P, decreases binding of VraR to the R1 and R2 sites (Figure 3C). This binding model is also supported by our earlier observations that the presence of P_{vraSR} increases the resistance of VraR to proteolysis (*5*). On the other hand, we believe that binding of VraR to the R2 site requires phosphorylation for two main reasons. First, the VraR-binding sequence is not conserved in R2, which results in a ∼4-fold decrease in the binding affinities of VraR and VraR∼P for R2 in comparison to R1. Second, the two VraR-binding sequences (R2a and R2b) are farther apart than in R1 (separated by four nucleotides instead of one), and the possibility that both monomers may come in contact with each other, on their own, is small. Both of these less-than-optimum binding conditions could be overcome if VraR is mobilized into a dimer prior to the binding of the target DNA.

Phosphorylation-dependent binding of VraR to the R2 site is centered at the −35 box. On the other hand, the DNA sequence at the −10 box (TTATAA) is very similar to the sequence recognized by *E. coli* σ^{70} factor (*20*, *21*). Analysis of the *S. aureus* genome has indicated that this organism contains a single primary σ factor, SigA (σ^A) (*22*), which is a homologue to *E. coli* σ^{70}. It is possible that protein−protein interactions between VraR-P at −35 and the σ^A of RNA polymerase could play a role in the transcriptional activation mechanism of VraR. Potential involvement of response regulatory proteins in recruiting or interacting with the σ factors has been recognized before, e.g., in the cases of PhoR, BvgA, and VanR (*15*−*17*). However, we cannot exclude the possibility that the recruitment of VraR-P to the −35 site may allow protein−protein interactions with VraR bound at the R1 and/or R3 sites, which may in turn cause DNA looping and facilitate potential interactions between σ^A of RNAP and upstream P_{vraSR} elements. This putative regulatory mechanism has been predicted for several RRs, e.g., Lrp on the *ilvIH* promoter (*23*), MalT on the *malPQ* promoter (*24*), FIS regulator on the *tyrT* promoter (*25*), OmpR on the *ompF* promoter (*26*), and PhoB on the *pstS* promoter (*27*), and it infers that there is cooperativity in binding between the VraR binding sites. Incidentally, the binding affinity of VraR∼P for P_{vraSR} was previously reported to be 1.4 μM, which is about 2- and 14-fold better than its binding affinities for R1 and R2, respectively (*5*), suggesting a potential cooperativity between these sites.

The binding affinity of VraR to R2 is low (K_d = 18 ± 2 μM); thus it is very unlikely to be occupied *in vivo* by unphosphorylated VraR. This situation suggests that only under conditions of cell

wall stress will this site be occupied by VraR, as VraR-P, and that only under these conditions will the *vraSR* operon be expressed at higher levels. The question that arises is then what is the role of the R1 site other than recruiting VraR to the promoter region? It is possible that under nonstress conditions binding of VraR to the R1 site may mediate basal expression of the *vraSR* operon, but for the expression of larger amounts of VraR that are necessary to activate the *vraSR* regulon (stress conditions) VraR must be recruited to the R2 site. This proposal fits well with the report by Kuroda et al. (*2*), whereby the inactivation of *vraSR* results in a substantial decrease of *pbpB* and *sgtB* (*2*, *28*) basal expressions.[2] Studies with other response regulators have shown that these proteins may interact with other elements of RNAP, such as the C-terminal domain of the α subunit of RNAP (αCTD) (*16*, *29*). We speculate that VraR, when bound at R1 under nonstress conditions, could interact with αCTD either through protein−protein interaction or by altering the topology of the DNA to enable basal expression of the *vraSR* operon.

In summary, our study shows that VraR binds to its promoter at three distinct sites. Binding of VraR to the R1 site displays the highest affinity. The presence of two putative VraR-binding sequences in tandem inverted repeats, separated by one nucleotide and oriented tail to tail (as in R1), could induce activation of the VraR in a phosphorylation-independent mechanism. Also, the data indicate that there is directionality into the binding of VraR with cytosine probably serving as an anchor point. Further, mutagenesis studies suggest that the role of phosphorylation is to enable VraR binding to the R2 site, the low-binding affinity site that overlaps with the −35 region. The lack of conservation of the VraR-binding sequence at this site suggests that it could enable discrimination between stress and nonstress conditions. We propose that, under nonstress conditions, unphosphorylated VraR occupies only the highest binding affinity site and this is sufficient to mediate basal levels of *vraSR* expression necessary for the cell to multiply; under stress conditions, VraR-P will be recruited to the lower binding affinity site to mediate a higher level of gene expression. The proposed regulatory mechanism for the *vraSR* operon could be employed for other genes within the *vraSR* regulon, although we cannot exclude the possibility of different regulatory mechanisms.

ACKNOWLEDGMENT

We are indebted to Dr. David Heinrichs for providing us with the pXEN1 plasmid.

SUPPORTING INFORMATION AVAILABLE

One table showing the primers used for the amplification of the target DNA sequences. This material is available free of charge via the Internet at http://pubs.acs.org.

REFERENCES

1. Kuroda, M., Kuwahara-Arai, K., and Hiramatsu, K. (2000) Identification of the up- and down-regulated genes in vancomycin-resistant *Staphylococcus aureus* strains Mu3 and Mu50 by cDNA differential hybridization method. *Biochem. Biophys. Res. Commun. 269*, 485–490.
2. Kuroda, M., Kuroda, H., Oshima, T., Takeuchi, F., Mori, H., and Hiramatsu, K. (2003) Two-component system VraSR positively modulates the regulation of cell-wall biosynthesis pathway in *Staphylococcus aureus*. *Mol. Microbiol. 49*, 807–821.
3. Boyle-Vavra, S., Yin, S., and Daum, R. S. (2006) The VraS/VraR two-component regulatory system required for oxacillin resistance in community-acquired methicillin-resistant *Staphylococcus aureus*. *FEMS Microbiol. Lett. 262*, 163–171.
4. Gardete, S., Wu, S. W., Gill, S., and Tomasz, A. (2006) Role of VraSR in antibiotic resistance and antibiotic-induced stress response in *Staphylococcus aureus*. *Antimicrob. Agents Chemother. 50*, 3424–3434.
5. Belcheva, A., and Golemi-Kotra, D. (2008) A close-up view of the VraSR two-component system. A mediator of *Staphylococcus aureus* response to cell wall damage. *J. Biol. Chem. 283*, 12354–12364.
6. Yin, S., Daum, R. S., and Boyle-Vavra, S. (2006) VraSR two-component regulatory system and its role in induction of pbp2 and vraSR expression by cell wall antimicrobials in *Staphylococcus aureus*. *Antimicrob. Agents Chemother. 50*, 336–343.
7. Donaldson, L. W. (2008) The NMR structure of the *Staphylococcus aureus* response regulator VraR DNA binding domain reveals a dynamic relationship between it and its associated receiver domain. *Biochemistry 47*, 3379–3388.
8. Gao, R., Mack, T. R., and Stock, A. M. (2007) Bacterial response regulators: versatile regulatory strategies from common domains. *Trends Biochem. Sci. 32*, 225–234.
9. Tran, V. K., Oropeza, R., and Kenney, L. J. (2000) A single amino acid substitution in the C terminus of OmpR alters DNA recognition and phosphorylation. *J. Mol. Biol. 299*, 1257–1270.
10. Gardner (2002) Acyclic and dideoxy terminator preferences denote divergent sugar recognition by archaeon and Taq DNA polymerases. *Nucleic Acids Res. 15*, 605–613.
11. Francis, K. P., Joh, D., Bellinger-Kawahara, C., Hawkinson, M. J., Purchio, T. F., and Contag, P. R. (2000) Monitoring bioluminescent *Staphylococcus aureus* infections in living mice using a novel *luxABCDE* construct. *Infect. Immun. 68*, 3594–3600.
12. Steidl, R., Pearson, S., Stephenson, R. E., Ledala, N., Sitthisak, S., Wilkinson, B. J., and Jayaswal, R. K. (2008) *Staphylococcus aureus* cell wall stress stimulon gene-lacZ fusion strains: potential for use in screening for cell wall-active antimicrobials. *Antimicrob. Agents Chemother. 52*, 2923–2925.
13. Schenk, S., and Laddaga, R. A. (1992) Improved method for electroporation of *Staphylococcus aureus*. *FEMS Microbiol. Lett. 73*, 133–138.
14. Maris, A. E., Sawaya, M. R., Kaczor-Grzeskowiak, M., Jarvis, M. R., Bearson, S. M., Kopka, M. L., Schroder, I., Gunsalus, R. P., and Dickerson, R. E. (2002) Dimerization allows DNA target site recognition by the NarL response regulator. *Nat. Struct. Biol. 9*, 771–778.
15. Paul, S., Birkey, S., Liu, W., and Hulett, F. M. (2004) Autoinduction of *Bacillus subtilis* phoPR operon transcription results from enhanced transcription from EsigmaA- and EsigmaE-responsive promoters by phosphorylated PhoP. *J. Bacteriol. 186*, 4262–4275.
16. Boucher, P. E., Murakami, K., Ishihama, A., and Stibitz, S. (1997) Nature of DNA binding and RNA polymerase interaction of the *Bordetella pertussis* BvgA transcriptional activator at the fha promoter. *J. Bacteriol. 179*, 1755–1763.
17. Depardieu, F., Courvalin, P., and Kolb, A. (2005) Binding sites of VanRB and sigma70 RNA polymerase in the vanB vancomycin resistance operon of *Enterococcus faecium* BM4524. *Mol. Microbiol. 57*, 550–564.
18. Martinez, B., Zomer, A. L., Rodriguez, A., Kok, J., and Kuipers, O. P. (2007) Cell envelope stress induced by the bacteriocin Lcn972 is sensed by the lactococcal two-component system CesSR. *Mol. Microbiol. 64*, 473–486.
19. Jordan, S., Junker, A., Helmann, J. D., and Mascher, T. (2006) Regulation of LiaRS-dependent gene expression in *Bacillus subtilis*: identification of inhibitor proteins, regulator binding sites, and target genes of a conserved cell envelope stress-sensing two-component system. *J. Bacteriol. 188*, 5153–5166.
20. Deora, R., and Misra, T. K. (1996) Characterization of the primary sigma factor of *Staphylococcus aureus*. *J. Biol. Chem. 271*, 21828–21834.
21. Deora, R., Tseng, T., and Misra, T. K. (1997) Alternative transcription factor sigmaSB of *Staphylococcus aureus*: characterization and role in transcription of the global regulatory locus sar. *J. Bacteriol. 179*, 6355–6359.
22. Kullik, I. I., and Giachino, P. (1997) The alternative sigma factor sigmaB in *Staphylococcus aureus:* regulation of the sigB operon in response to growth phase and heat shock. *Arch. Microbiol. 167*, 151–159.

[2]The expression of these genes is necessary for normal cell multiplication; *pbpB* encodes for the penicillin-binding protein 2 (PBP2), which is involved in the last step of peptidoglycan synthesis, and *sgtB* is suggested to encode for a soluble transglycosylase that may participate in cell division.

23. Wang, Q., and Calvo, J. M. (1993) Lrp, a major regulatory protein in *Escherichia coli*, bends DNA and can organize the assembly of a higher-order nucleoprotein structure. *EMBO J. 12*, 2495–2501.
24. Danot, O., and Raibaud, O. (1994) Multiple protein-DNA and protein-protein interactions are involved in transcriptional activation by MalT. *Mol. Microbiol. 14*, 335–346.
25. Muskhelishvili, G., Travers, A. A., Heumann, H., and Kahmann, R. (1995) FIS and RNA polymerase holoenzyme form a specific nucleoprotein complex at a stable RNA promoter. *EMBO J. 14*, 1446–1452.
26. Mattison, K., Oropeza, R., Byers, N., and Kenney, L. J. (2002) A phosphorylation site mutant of OmpR reveals different binding conformations at *ompF* and *ompC*. *J. Mol. Biol. 315*, 497–511.
27. Makino, K., Amemura, M., Kawamoto, T., Kimura, S., Shinagawa, H., Nakata, A., and Suzuki, M. (1996) DNA binding of PhoB and its interaction with RNA polymerase. *J. Mol. Biol. 259*, 15–26.
28. Pinho, M. G., Filipe, S. R., de Lencastre, H., and Tomasz, A. (2001) Complementation of the essential peptidoglycan transpeptidase function of penicillin-binding protein 2 (PBP2) by the drug resistance protein PBP2A in *Staphylococcus aureus*. *J. Bacteriol. 183*, 6525–6531.
29. Olekhnovich, I. N., and Kadner, R. J. (1999) RNA polymerase alpha and sigma(70) subunits participate in transcription of the *Escherichia coli* uhpT promoter. *J. Bacteriol. 181*, 7266–7273.
30. Roberts, D. M., Liao, R. P., Wisedchaisri, G., Hol, W. G., and Sherman, D. R. (2004) Two sensor kinases contribute to the hypoxic response of *Mycobacterium tuberculosis*. *J. Biol. Chem. 279*, 23082–23087.
31. Ferrieres, L., and Kahn, D. (2002) Two distinct classes of FixJ binding sites defined by *in vitro* selection. *FEBS Lett. 517*, 185–189.
32. Vannini, A., Volpari, C., Gargioli, C., Muraglia, E., Cortese, R., De Francesco, R., Neddermann, P., and Marco, S. D. (2002) The crystal structure of the quorum sensing protein TraR bound to its autoinducer and target DNA. *EMBO J. 21*, 4393–4401.
33. Yoshida, T., Qin, L., Egger, L. A., and Inouye, M. (2006) Transcription regulation of *ompF* and *ompC* by a single transcription factor, OmpR. *J. Biol. Chem. 281*, 17114–17123.
34. Kato, A., Tanabe, H., and Utsumi, R. (1999) Molecular characterization of the PhoP-PhoQ two-component system in *Escherichia coli* K-12: identification of extracellular Mg^{2+}-responsive promoters. *J. Bacteriol. 181*, 5516–5520.